Solvation of the *N*-(1-Phenylethyl)-*N*′-[3-(triethoxysilyl)propyl]-urea Chiral Stationary Phase in Mixed Alcohol/Water Solvents

Sorin Nita, J. Hugh Horton, and Natalie M. Cann*

Department of Chemistry, Queen's University, Kingston, Ontario, Canada K7L 3N6

Received: December 9, 2005; In Final Form: March 14, 2006

A theoretical and experimental study of alcohol/water and alcohol/alcohol solvent mixtures near a surface of *N*-(1-phenylethyl)-*N*′-[3-(triethoxysilyl)propyl]-urea (PEPU), a Pirkle-type chiral stationary phase, is presented. Molecular dynamics simulations are performed at room temperature for water/methanol, water/1-propanol, water/2-propanol, and methanol/1-propanol solvent mixtures confined between two PEPU surfaces. The interface was also prepared experimentally by attaching the PEPU molecules to atomic force microscopy tips and oxidized Si(111) substrates. Chemical force spectrometric measurements between such PEPU-terminated tips and samples were taken in the solvent mixtures, and the results are compared to the molecular dynamics study. We find that the extent of hydrogen bonding at the surface is the dominant contributor to the measured forces.

1. Introduction

Water/alcohol binary mixtures are often used as solvents in chemical processes and have many industrial applications. In mixtures of low molecular weight alcohols and water, the two components are completely miscible. Many experimental and theoretical studies suggest a complex structural arrangement in water/alcohol mixtures. A significant self-association of alcohols in water was observed in NMR,[1] IR absorption,[2] thermodynamic,[3] and neutron diffraction[4] studies. In water−alcohol mixtures, hydrogen bonds are formed between water and alcohol molecules,[5,6] the water−water hydrogen bonding networks are fully percolating at low alcohol concentrations,[7] while evidence suggests that water clusters appear at high alcohol concentrations.[8−10]

In typical chromatography, the mobile phase is a mixture of organic solvents that mediate the interaction of the solvated components and the stationary phase. Because of this, understanding the mechanism by which the mixture of solvents interacts with the solid stationary phase is of critical importance. The reagent of interest in this article is (*S*/*R*)-*N*-(1-phenylethyl)-*N*′-[3-(triethoxysilyl)propyl]-urea or PEPU.[11] PEPU may be readily covalently bonded to silica particles through a hydrolysis reaction. The resulting stationary phase is a typical Type I, or Pirkle,[12] chiral stationary phase (CSP), where a chiral end group is attached, via an amide or ether linker, to the siloxane "tether". A siloxane linkage is then used to attach the tether to the surface of a silicate particle. The PEPU interface also contains other features common to Type I CSPs: the presence of phenyl groups that may undergo stacking interactions and sites (in this case within the urea group) that may undergo hydrogen bonding in solution. A PEPU-based CSP has been used to chromatographically separate the isocyanate and isothiocyanate derivatives of (*S*/*R*)-propranolol[13,14] in a mixed solvent of *n*-hexane, 2-propanol, and acetonitrile.

The role of the solvent is precisely the objective of this article: we wish to obtain a clear understanding of solvent distribution, solvent density, hydrogen bonding, and solvent orientation at the fluid−CSP boundary. Several recent articles[12,15−17] summarize techniques available for atomistic modeling of chiral interfaces. Briefly, modeling is restricted to ab initio or force field calculations for noncovalently bonded CSP−analyte complexes in the absence of solvent. Unfortunately most CSPs do not form inclusion complexes where, to a first approximation, the solvent can be ignored. Alternatively, structure−function relationships[18,19] use experimental results for related analytes expressed in terms of molecular descriptors. After sophisticated regression, one arrives at a compact set of descriptors that reproduce elution orders and enantioseparation factors and have predictive power for related analytes. A representation of the CSP *and* solvent is included in this approach but only at an implicit level. In this article, we focus specifically on the solvent and perform detailed molecular dynamics simulations of the interface between PEPU and binary water/alcohol and alcohol/alcohol solvents.

The choice of solvent has a strong effect on the interaction forces observed in a chemical force spectrometric measurement. In systems where the pull-off forces between two hydrophobic surfaces are measured in aqueous solution[20] the forces observed are often very large and highly dependent on the ionic strength of solution, suggesting that solvation effects play a key role in the tip−sample interaction. It has been noted that[21] the interfacial free energy between the probe and substrate must dominate that of either the probe/solvent or substrate/solvent in order to achieve discrete sensitivity to chemical bonds formed in the contact between tip and sample. We have previously studied the PEPU interface in the presence of water, methanol, and CS_2.[11] The PEPU molecules were self-assembled both on an oxidized Si(111) surface and on an oxidized Si_3N_4 atomic force microscopy (AFM) tip, through a hydrolysis reaction onto silanol (Si−OH) sites. By use of chemical force microscopy (CFM), we measured the adhesive interactions between the tip and sample in the three pure solvents and showed that, in methanol, chiral discrimination could be observed experimentally between the PEPU molecules on the tip and sample. However, when water was used as a solvent, the overall forces observed were

* To whom correspondence should be addressed. Telephone 613-533-2651; FAX 613-533-6669; e-mail ncann@chem.queensu.ca.

10.1021/jp057204s CCC: $33.50
Published on Web 04/21/2006

much higher than in methanol, and no chiral discrimination could be observed. Molecular dynamics (MD) simulations on these model CSP systems showed that the density and degree of association of the solvent were determining factors in the selection process.

In this article, the solvation of the PEPU interface is examined for 36 binary solvent mixtures. These consist of methanol/water, 1-propanol/water, 2-propanol/water, and methanol/1-propanol mixtures with the alcohol mole fraction ranging from 0 to 1.0. The comparison between these alcohols is interesting because they have virtually identical gas-phase dipole moments but their dielectric constants vary from 32.6 for methanol to 18.3 for 2-propanol.[22] The solvation of PEPU interfaces in the binary solvents is modeled by MD simulations to provide a molecular level description of the solvent characteristics at the surface. We correlate these results to chemical force spectrometric measurements of the overall adhesive interaction between PEPU molecules and compare the structure and solvation in the various solvent mixtures.

2. Experimental and Computational Methods

2.1. Sample Preparation and AFM Measurements. Both oxidized Si(111) surfaces and oxide-sharpened silicon nitride cantilevers (Veeco Metrology LLC, Santa Barbara, CA) were functionalized with a chirally terminated surface by solution deposition from 1.0×10^{-3} mol L^{-1} in toluene of either (*R*)- or (*S*)-PEPU (95%, Gelest Inc., Tullytown, PA). Details of the deposition procedure and characterization of the PEPU layers formed have been described previously.[11]

AFM and CFM data were acquired using a PicoSPM (Molecular Imaging, Tempe, Arizona) using a Nanoscope IIE controller (Digital Instruments, Santa Barbara, CA). For the acquisition of force−displacement curves, a chemically modified tip and corresponding sample were immersed in the appropriate solvent mixture. To have the CFM data in approximately the same spot of the sample for all the runs, the entire tip−sample ensemble was introduced into a small cell that can be filled with the desired solvent mixture. The solvent mixture can therefore be easily removed and another can be introduced in the cell while the tip is still very close to the surface. A series of 150−250 force curves was obtained for each sample−tip combination. The average values of the adhesive interaction are reported while the errors reflect the standard deviation of the data. The force constants of the AFM tips used here were calibrated based on the cantilever geometry using the method of Sader et al.[23−26] and ranged from about 0.1 N m^{-1} to 0.15 N m^{-1}, within the manufacturer's specifications.

2.2. MD Simulations. MD simulations of the chiral interface require an atomic level description of the PEPU molecules. A realistic model was previously constructed[11] based on a series of B3LYP/6-31G* calculations using the Gaussian 98 program.[27] Briefly, the calculations indicated that neighboring PEPU molecules align themselves to form energetically favorable hydrogen bonds between the tethers. On the basis of these results and with the mesostructure of the silicon surface in mind, a model CSP consisting of a closely packed, regular monolayer of PEPU molecules was constructed. Each PEPU molecule is charge neutral although the constituent atoms bear partial charges and the dipole moment is 3.3 D. Since the PEPU molecules are closely spaced and interconnected with hydrogen bonds, the model surface is kept rigid throughout the simulations. The solvent accessible portion of the surface consists of a regular array of aromatic rings, each ring being the topmost segment of a PEPU molecule. The polar urea segment is directly below the aromatic group, rendering the nature of the full surface complex: hydrophobic groups directly exposed to solvent and polar groups further away. The PEPU monolayer is placed above two layers of silicon with a silicon−silicon distance of 3 Å. Full details of the PEPU model, as employed in the simulations, are given elsewhere.[11]

The solvent mixtures under consideration consist of water/methanol, water/1-propanol, water/2-propanol, and methanol/1-propanol. Thus, representations of water and three alcohols are required in the simulations. The three-point F3C model of water[28] was chosen. This nonpolarizable flexible model has been used extensively in recent years, notably for biomolecular simulations,[29,30] but it has also been employed to study methanol/water mixtures[31−33] and for investigation of Au−water interfaces.[34,35] The F3C model compares favorably with other models, as highlighted by two recent and extensive comparisons between water models, for bulk properties[36] and for solvated biomolecules.[37] For the alcohols, we required transferable models with functional forms paralleling the representation of water. The TraPPE-UA (transferable potential for phase equilibria united atoms) alcohol models developed by Chen et al.[38] were chosen. The TraPPE-UA model has been extensively tested for phase equilibria (vapor−liquid coexistence curves) and fluid structure.[38] In addition, this model has been used in recent simulations of alcohol/water mixtures.[39,40] In preliminary simulations of the PEPU interface, we allowed bending and torsional motion in the solvent. An analysis of the results showed that bending motion was limited but that torsional degrees of freedom are particularly important in understanding the molecular orientation of the alcohols at the PEPU surface. Consequently, bond lengths and angles were kept fixed in the subsequent simulations, but torsional motion was allowed.

The full simulation cell is a rectangular prism and includes *two* well-separated surfaces, as is often done[41] for simulations of interfaces. The surfaces, including the underlying silicon atoms, are roughly 14.6 Å thick and are positioned perpendicular to the *z* axis of the cell. The intersurface distance depends on the fluid density and the number of solvent molecules included in the simulation. The simulation cell also includes empty space, above and below the surfaces, to eliminate any interactions between the surface−fluid−surface periodic images. The dimensions of the full rectangular prism cell are 30 Å × 30 Å × 360 Å for all water/alcohol simulations. A slightly more elongated cell is used for the methanol/1-propanol simulations: 30 Å × 30 Å × 400 Å. With these dimensions, our simulation cells are 12−13 times longer in the *z* direction than along the *x* and *y* axes. In contrast, the intersurface distance is 2−4 times the side length of the cell. Ewald[42] summations, for a cell replicated in 3D, are used to treat the long-ranged Coulombic forces between charged sites. All results below correspond to conducting boundary conditions ($\epsilon = \infty$), a position space cutoff of $\alpha L_x = 7.175$ and a momentum space cutoff of $k^2 = 27.0/L_x^2$.

The simulations are performed at 298 K and at the experimental densities[43] (see Supporting Information for details). A Nose−Hoover thermostat[44] is used to generate canonical (NVT) averages. The algorithm described by Martyna et al.[45] is used to integrate the Nose−Hoover equations of motion, so that the RATTLE constraints are met. Each MD simulation follows the evolution of the interface for 100 000 time steps, with each step corresponding to 0.25 fs. Equilibration of the fluid occurs within the first 20 000 time steps, and statistics are compiled for the remaining 80 000 steps. For each of the four solvent mixtures, 9 compositions are considered, giving a total of 36 interfacial

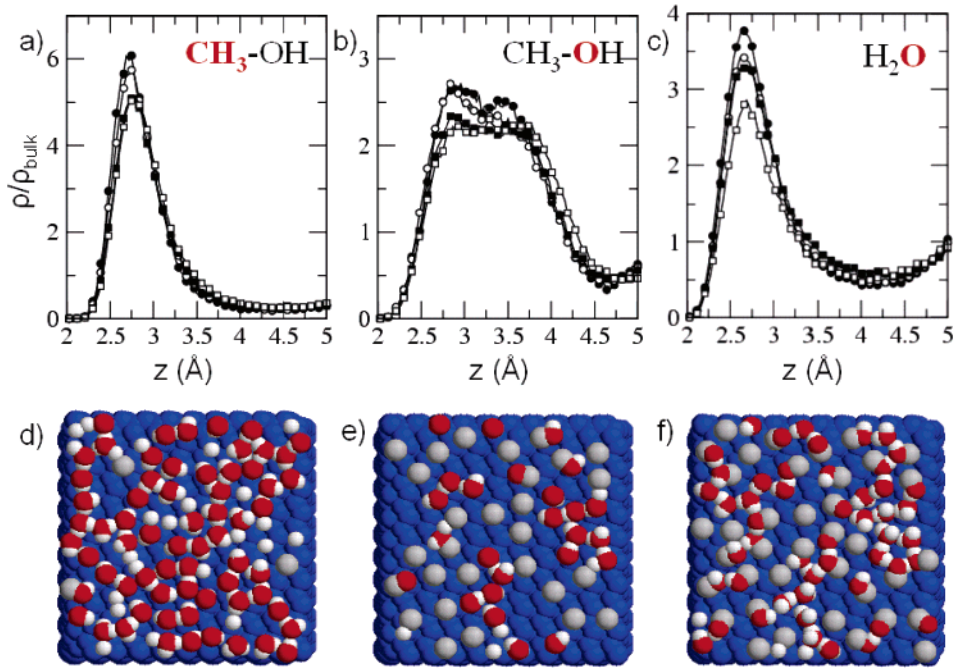

Figure 1. Density profiles and snapshots from water/methanol simulations. Distances are measured relative to the position of the topmost PEPU atom ($z = 0$). Density profiles for the methyl group, the alcohol oxygen, and the water oxygen, are shown in (a), (b), and (c), respectively. The full circles, empty circles, full squares, and empty squares correspond to the mixtures with methanol mole fractions 0.123, 0.273, 0.457, and 0.692, respectively. Snapshots of the molecules found within 3 Å (d, e), and 4 Å (f) above the topmost PEPU are also shown. In (d) the methanol mole fraction is 0.059; for (e) and (f) the methanol mole fraction is 0.567. The oxygen, hydrogen, alkyl carbon are indicated in red, white, and gray, respectively. The atomic positions of the underlying PEPU are shown in blue.

fluids. Between the surfaces, 1 000 solvent molecules are included in the simulations. This relatively large number is required to ensure the accuracy of the surface distribution of molecules. We require that the distance between the center of the simulation cell and the topmost PEPU atom exceeds four solvent diameters. In this way, molecules at the center of the cell are "far" from either surface. The results presented for each fluid summarize 5 independent simulations, with 2 interfaces per simulation, for a total of 10 interfaces for each binary solvent. All simulations are performed with the MDMC program.[46]

Our procedure for generating an initial configuration consists of the following steps. First, an excess of solvent molecules (1 372) are placed on a rectangular prism lattice, then molecules are removed at random until 1 000 remain. Molecular identities for the remaining 1 000 solvent molecules are assigned at random but are constrained to be consistent with the mole fraction of interest. The molecules are assigned random orientations. After that, the simulation cell is expanded (in 5% increments of the boxlength) until strong overlaps are removed (average potential energy is less than 1.0 in reduced units). The recompression of the simulation cell includes Monte Carlo (MC) cycles, where a cycle consists of 10 000 attempted moves (translation and rotation) at an elevated temperature of 450 K. Specifically, Monte Carlo cycles are performed until two consecutive cycles predict potential energies within 8% of each other. The simulation cell is then compressed (boxlength is reduced by 5%) and the Monte Carlo cycles are repeated until two consecutive potential energies are again within 8%. The compression-plus-MC iterative cycle is completed when the desired density is recovered, provided a minimum of 25 MC cycles have been performed. Then the molecules are assigned random linear velocities and angular velocities, consistent with the temperature of interest (298 K). This elaborate initialization procedure is time consuming, but the use of random numbers throughout ensures that the resulting initial configurations are highly distinct.

To explore the details of the solvent structure near the PEPU interface, molecules within 5 Å of the topmost PEPU atom, on either surface, were counted throughout the collection period of the simulation, at 20 iteration intervals. The atomic positions for each of these molecules were recorded to provide information on molecular orientation and hydrogen bonding at the surface. For comparison, atomic positions are also collected for molecules located within 5 Å of the center of the simulation cell. From these data, density profiles, snapshots, molecular distributions and orientations, and hydrogen bonding at the surface are evaluated and reported in section 3.1.

3. Results and Discussion

3.1. Solvation of the PEPU Interface. Figure 1 shows snapshots and density profiles for several water/methanol mixtures near the PEPU interface. Density profiles are collected by comparing the number of atoms found a distance z above the surface, relative to the number expected from the bulk density (ideal solvent). From the density profiles shown in Figure 1, a methyl group has a high probability of being within 2.5−3.0 Å of the topmost carbon atom of PEPU. In contrast, the alcohol oxygen distribution is broad, with a peak evident at roughly 2.8 Å above the surface and a second peak at roughly 3.7 Å. The first peak corresponds to oxygen atoms in contact with the surface and, from Figure 1b, the probability for contact decreases somewhat as the solvent becomes methanol rich. Relative to methanol, the oxygen atom from water is localized within 2.5−3.0 Å of the surface. The snapshot in Figure 1d shows all atoms within 3.0 Å of the surface for a predominantly water solvent. The water molecules prefer to form four- and five-membered hydrogen bonded rings that lie flat on the surface. When methanol accounts for a larger fraction of the

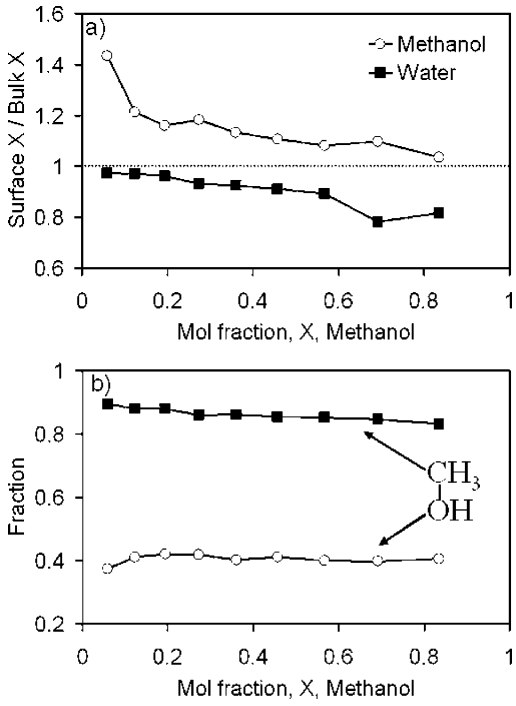

Figure 2. Relative distributions of water and methanol molecules at the PEPU/solution interface: (a) surface-to-bulk mole fraction ratios for methanol and water; (b) the fraction of methanol molecules at the surface with methyl or hydroxyl groups that lie within the surface layer (0−3 Å above the PEPU layer).

solvent (parts e and f of Figure 1), these ring structures are less evident at the surface but the water molecules still prefer to aggregate, forming at least one hydrogen bond parallel to the surface. The methanol molecules also participate in hydrogen bonding, and some molecules lie flat on the surface (Figure 1e), but they typically orient the OH group toward the bulk. This may be seen by comparing the snapshots from parts e and f of Figure 1 that show the atoms 3 and 4 Å above the surface, respectively. For most of the molecules only the methyl group is usually found within 3 Å of the surface.

The behavior of water and methanol near the PEPU surface can be understood by comparing their surface mole fraction with the mole fraction in the bulk liquid (Figure 2). For the purposes of defining a surface mole fraction, a molecule is counted if any atom belonging to that molecule is found within 3 Å of the topmost PEPU atom. Figure 2a shows the surface mole fraction of methanol and water, as a function of the bulk composition. Water prefers to reside in the bulk while the surface concentration of methanol is enhanced relative to the bulk. These results suggest that the networked water structure can be disrupted even by a small number of methanol molecules. Once this disruption occurs, the hydrogen bonding between waters on the surface is less favorable and the water prefers the bulk. The presence of methanol-rich surface domains and partially formed networks of water, are evident in the snapshots (parts e and f of Figure 1) and clearly show this disruption. Figure 2b shows the fraction of surface methanol molecules with an oxygen or a methyl group within 3 Å of the surface. Note that the fractions do not add up to unity since molecules in which both oxygen and methyl groups lie within 3 Å of the surface (i.e., lying parallel to the surface) are counted twice. From the figure, virtually all of the methanol molecules prefer to place the methyl group near the surface, and most point the hydroxyl group toward the bulk.

Density profiles and snapshots for 1-propanol/water mixtures are presented in Figure 3. The profiles are similar to the methanol/water profiles (Figure 1) except that the oxygen from 1-propanol has a broader distribution near the surface and the double-peak structure present for methanol (Figure 1b) is less evident. The peak in the density profile for the water oxygen also tends to be slightly higher for 1-propanol/water mixtures. Snapshots of molecules within 3 Å of the surface (parts d and

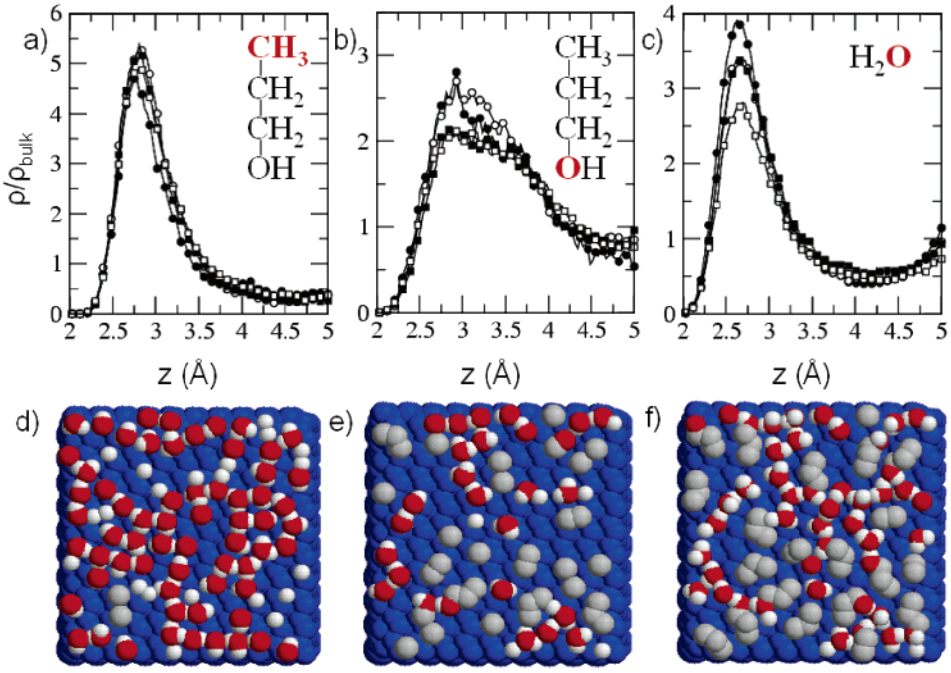

Figure 3. Density profiles and snapshots from water/1-propanol simulations. Distances are measured relative to the position of the topmost PEPU atom ($z = 0$). Density profiles for the methyl group, the alcohol oxygen, and the water oxygen, are shown in (a), (b), and (c), respectively. The full circles, empty circles, full squares, and empty squares correspond to the mixtures with 1-propanol mole fractions 0.07, 0.167, 0.31, and 0.545, respectively. Snapshots of the molecules found within 3 Å (d, e), and 4 Å (f) above the topmost PEPU atom are also shown. For (d) the 1-propanol mole fraction is 0.032; for (e) and (f) the 1-propanol mole fraction is 0.412. The oxygen, hydrogen, alkyl carbon are indicated in red, white, and gray, respectively. The atomic positions of the underlying PEPU are shown in blue.

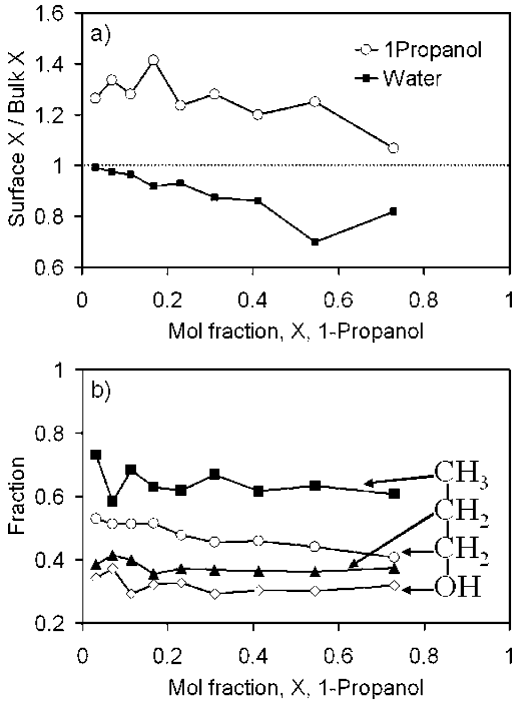

Figure 4. Relative distributions of water and 1-propanol molecules at the PEPU/solution interface: (a) surface-to-bulk mole fraction ratios for 1-propanol and water; (b) the fraction of 1-propanol molecules at the surface with methyl, methylene or hydroxyl groups that lie within the surface layer (0−3 Å above the PEPU layer).

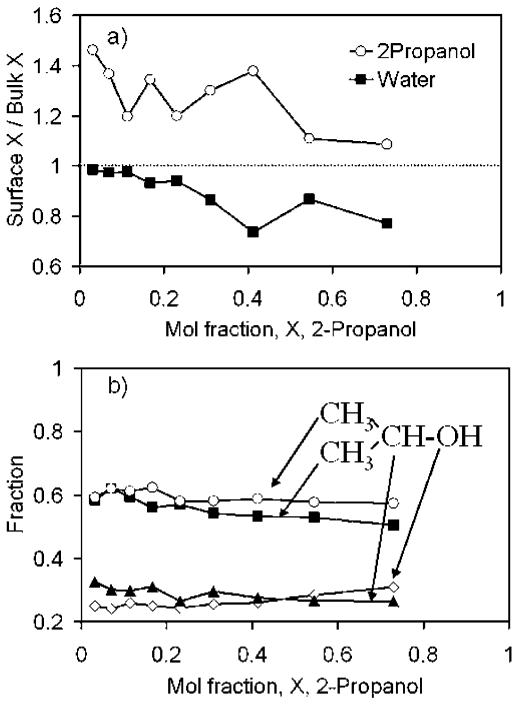

Figure 5. Relative distributions of water and 2-propanol molecules at the PEPU/solution interface: (a) surface-to-bulk mole fraction ratios for 2-propanol and water; (b) the fraction of 2-propanol molecules at the surface with methyl, methine or hydroxyl groups that lie within the surface layer (0−3 Å above the PEPU layer).

e of Figure 3) show that the hydrogen-bonded water network is easily disrupted by the alcohol. 1-Propanol tends to form domains with the apolar portion of the molecule at the surface. Since 1-propanol is large relative to water, the intermolecular spacing is larger than for water, and the water−hydrogen bond network is disrupted more easily than for methanol/water mixtures. A comparison of parts d and e of Figure 3 shows that the alcohols form hydrogen bonds near the surface but they prefer to have their alkyl groups at the surface and form their hydrogen bonds 3−5 Å above the surface. A similar disruption of the water hydrogen bonding at the surface, and segregation, is observed for 2-propanol/water mixtures. Both 1- and 2-propanol displace water at the PEPU surface, as shown by the surface mole fractions (Figures 4a and 5a). The orientations of 1-propanol and 2-propanol at the PEPU surface are shown in Figures 4b and 5b, respectively. At all concentrations, the molecules tend to place the terminal methyl groups within 3 Å of the surface. The other groups are less frequently found near the surface and, relative to methanol, fewer molecules have their oxygen atoms within 3 Å of the surface. A preference for the trans molecular configuration means that the central carbon is often more than 3 Å away from the surface for 2-propanol (Figure 5b) and the surface fractions alternate for 1-propanol (Figure 4b).

The distinction between water and alcohol hydrogen bonding has been explored by Noskov et al.[7] for water/ethanol mixtures. They performed molecular dynamics simulations of mixtures of varying compositions and quantified the water/ethanol partitioning within the fluid. Their results indicate that water forms hydrogen-bonded clusters that have a large range of sizes. In particular, when the water mole ratio is 0.5, the probability distribution for cluster sizes is very broad: water clusters contain between 1 and 100 molecules. Overall, Noskov et al.[7] found that the fluid was more segregated into alcohol-rich and water-rich domains than one might expect for ethanol/water. We find

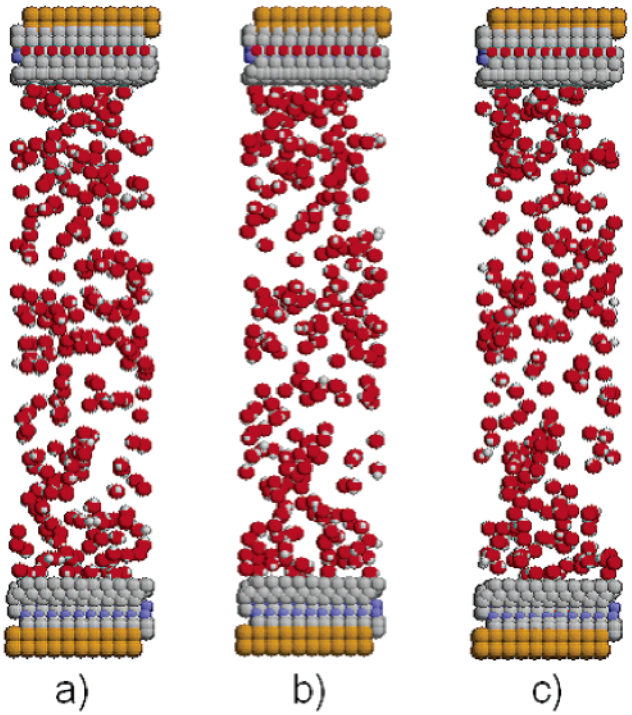

Figure 6. Side view of the simulation cell for the 2-propanol/water mixture where the 2-propanol mole fraction is 0.73 at different simulation times: 10.12 ps (a), 15.64 ps (b), and 21.16 ps (c). For clarity, only the water molecules are shown. The oxygen, nitrogen, carbon, and hydrogen are indicated in red, blue, gray, and white, respectively.

a similar segregation at the PEPU surfaces. Even at very low alcohol concentrations, only methanol is able to integrate into the water structure (Figure 1d). 1- and 2-propanol, by virtue of their size and conformational preferences, do not "fit" into the

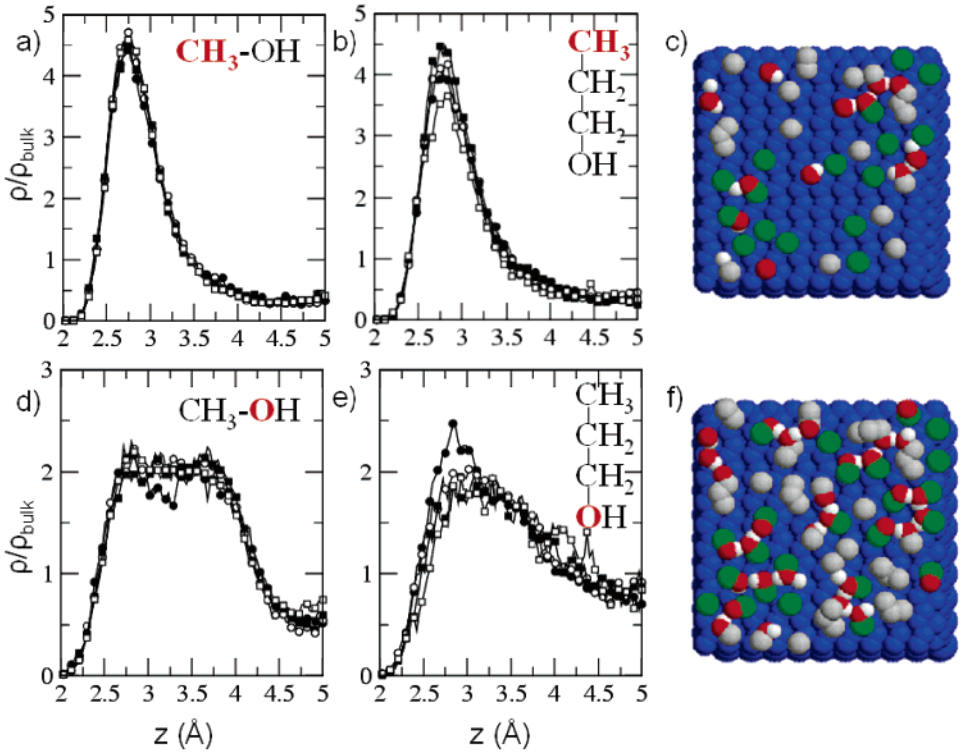

Figure 7. Density profiles and snapshots from methanol/1-propanol simulations. Distances are measured relative to the position of the topmost PEPU atom ($z = 0$). Density profiles of methyl group from 1-propanol, methyl group from methanol, oxygen from 1-propanol, and oxygen from methanol, are shown in (a), (b), (d), and (e), respectively. The full circles, empty circles, full squares, and empty squares correspond to the mixtures with methanol mole fractions 0.333, 0.56, 0.73, and 0.881, respectively. Snapshots of the molecules found within 3 Å and 4 Å above the topmost PEPU atom are shown in (c) and (f) for the methanol/1-propanol mixture with a methanol mole fraction 0.65. The oxygen, hydrogen, 1-propanol alkyl carbon, methanol carbon are indicated in red, white, gray, and green, respectively. The atomic positions of the underlying PEPU are shown in blue.

water structure at any concentration (parts d and e of Figure 3). As a result, the PEPU surface can be roughly divided into water-rich and alcohol-rich regions. Figure 6 shows snapshots of the entire simulation cell, highlighting the water molecules. Water clusters are clearly present in the snapshots. Similar segregation was proposed by Dixit et al.[8] in a recent neutron diffraction study.

To further explore the relationship between hydrogen bonding preferences and segregation, methanol/1-propanol simulations were performed. The density profiles (parts a, b, d, and e of Figure 7) show that both alcohols prefer to have a contact layer at about 2.8 Å above the surface formed mainly from their alkyl component. The oxygen location is less well defined but for methanol the oxygen distribution shows a double peak structure that is not present for 1-propanol. Snapshots of the contact layers show no clear indication of methanol or 1-propanol domains near the surface even at high concentrations of one of the alcohols (Figure 7c). In the absence of the water hydrogen bond network, the alcohols are more uniformly arranged. Figure 8a shows that the molecular distribution at the surface is equivalent (within statistics) to the bulk distribution. Note that the statistical error is highest for $X_{meth} = 0.945$ since the solvent only contains 55 1-propanol molecules and only a few are near a surface during each simulation. The relative orientation of the molecules in the contact layer is shown in parts b and c of Figure 8. Methanol and 1-propanol adopt similar orientations at the surface in alcohol/alcohol and alcohol/water mixtures.

By counting the number of hydrogen bonds in the 5 Å layer near the PEPU interface we can quantify the solvation effects at the surface. Following others,[7,47,48] we use a structural definition for hydrogen bonds: two molecules are considered to be hydrogen bonded if the H···O distance is less than 2.4 Å and the O−H···O angle is larger than 150°. In Figure 9 we observe that the total number of hydrogen bonds in methanol/water mixtures is larger than in either of the propanol/water mixtures at the same mole fraction. This is due to the larger number of hydrogen bonds formed by the alcohol in the methanol solutions. For example, at a methanol mole fraction of 0.36, only 40% of the total hydrogen bonds are water−water hydrogen bonds. In the propanol mixtures of similar concentration, this value has increased to 60%. In methanol/1-propanol mixtures the preference for hydrogen bonding increases with the mole fraction of methanol, presumably as the smaller molecule may more readily form hydrogen bonding networks. A hydrogen-bond analysis was also performed in the center of the simulation cell. The same overall trends with alcohol composition and concentration were observed, but a quantitative comparison between the number of hydrogen bonds at the surface and in the bulk is not possible since an accurate estimate of the solvent volume excluded by the structured PEPU surface is required.

3.2. Chemical Force Spectrometric Measurements. Force profiles for *R*-PEPU terminated tips on *S*-PEPU-terminated samples in a series of water/alcohol mixtures are shown in Figure 10a. The solvent mixtures experimentally used had the same compositions with those modeled using molecular dynamics simulations and discussed in section 3.1. Force profiles for the other chiral combinations (*R*/*R*, *S*/*S*, *S*/*R*) were also acquired giving similar results but without highlighting a clear chiral discrimination. As we have shown in a previous study,[11] the presence of water molecules in a solvent mixture tends to obscure the chiral discrimination effects. The well depth

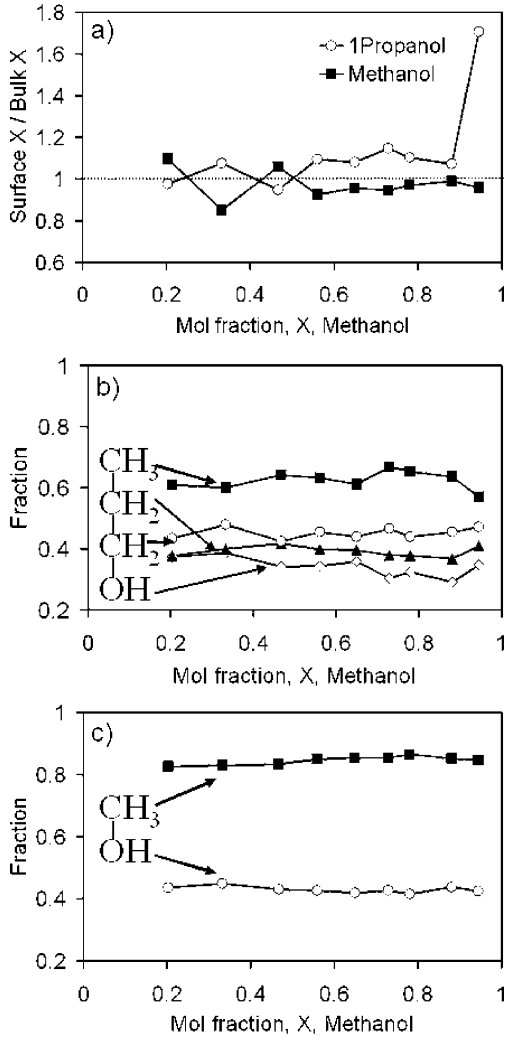

Figure 8. Relative distributions of methanol and 1-propanol molecules at the PEPU/solution interface: (a) surface-to-bulk mole fraction ratios for 1-propanol and methanol; the fraction of 1-propanol (b) and methanol (c) molecules at the surface with methyl, methylene or hydroxyl groups that lie within the surface layer (0−3 Å above the PEPU layer).

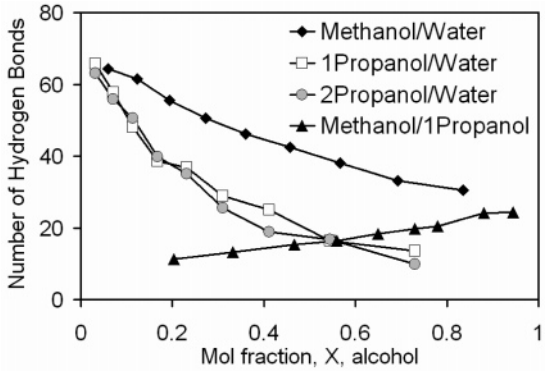

Figure 9. Number of hydrogen bonds in the 5 Å layer above the PEPU surface in methanol/water, 1-propanol/water, 2-propanol/water, and methanol/1-propanol mixtures as a function of the alcohol mole fraction (the methanol mole fraction is used for methanol/1-propanol mixtures).

obtained from the force-displacement curve as the tip was retracted from the surface was used to obtain the adhesive force between tip and sample. For any given solvent composition, the adhesive force reported was the average of between 150 and 250 such measurements. At high water concentrations, the adhesive forces between tip and sample were not highly reproducible.

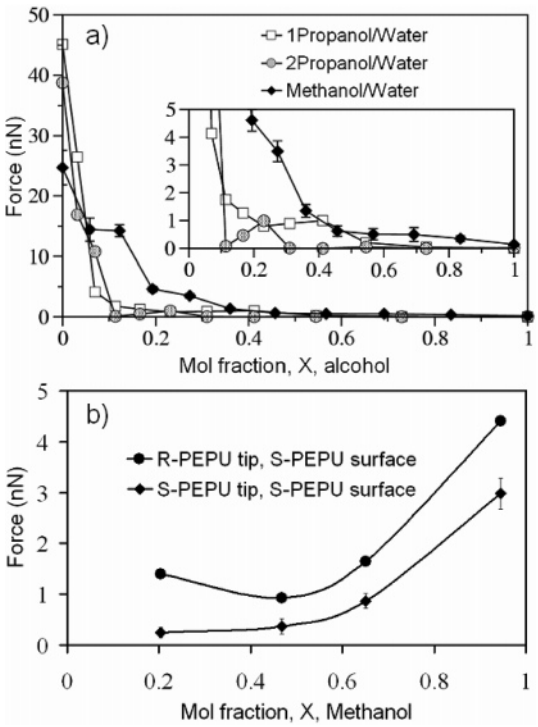

Figure 10. (a) Force curves obtained in water/alcohol mixtures between an *R*−PEPU tip and *S*−PEPU surface. (b) Force curves obtained in methanol/1-propanol mixtures for two combinations of R and S isomers of PEPU deposited on an AFM tip and an oxidized Si (111) surface. Typical error bars are shown on one curve. The errors reflect the standard deviation of the data acquired from 150 to 250 force curves for each mixture. Error bars on the remaining data are similar in magnitude but are omitted for clarity.

Despite the poor reproducibility at high water concentrations, some general trends may be observed in the data. In all cases, the magnitude of the adhesion force decreases with increasing alcohol concentration. With pure water as the solvent, the adhesive forces observed are on the order of 25−50 nN, similar to that previously reported.[11] This is reduced by an order of magnitude with pure alcohol as a solvent. In the mixtures where water is predominant, there is a high force interaction between the tip and the substrate as the hydrogen bonding network is disrupted at the interfacial region. In the alcohol rich mixtures, the force is significantly lowered as the hydrogen-bonding network is less pronounced. This is consistent with the molecular dynamics results, which showed a decline in the number of hydrogen bonds as the fraction of alcohol increases (Figure 9).

There is also a significant difference between the 1-propanol/water or 2-propanol/water force profile as compared with the methanol/water profile. The forces from 1- or 2-propanol/water mixtures decrease sharply at an alcohol mole fraction of about 0.1 and are very low (0−2 nN) for the higher alcohol fractions. Such a sharp decrease is not apparent for the methanol/water mixtures. The curves in Figure 10a decrease much more smoothly as the methanol fraction is increased. These results can be understood by considering the distribution of hydrogen bonding networks at the surface (compare the profiles of the curves in Figure 10a with those in Figure 9). 1- and 2-propanol are large molecules that prefer to have their hydrophobic alkyl groups near the surface. Thus, even at relatively low alcohol concentrations, the hydrogen-bonding network is strongly disrupted. As the tip/sample interaction appears to be strongly controlled by the extent of the hydrogen-bonding network at

the interface, this leads to the lower adhesive forces observed. For example, from Figure 9 one may note that a 1-propanol mole fraction of just 0.2 in water is sufficient to nearly halve the number of hydrogen bonds at the surface. In Figure 10a, we observe that, at the same concentration of 1-propanol, the adhesive interaction has dropped to <5% of its value in pure water. As a smaller molecule, methanol is more predisposed to form hydrogen bonds to other methanol molecules or to water molecules. Indeed, we see that, for methanol/water mixtures in Figure 9, methanol mole fractions in excess of 0.6 are required to halve the number of hydrogen bonds at the interface, as compared to pure water. This may be compared to Figure 10, which shows that the adhesive interactions drop off relatively slowly. Thus, the hydrogen-bonding network remains intact over a much wider range of methanol/water compositions, leading to a much more gradual decrease in adhesive interaction as the methanol concentration is increased.

In methanol/1-propanol mixtures the forces observed between a PEPU-terminated tip and a PEPU-terminated surface are much smaller that those found in the water/alcohol mixtures. These forces range from 0 to 5 nN (Figure 10b) and are comparable to the adhesive forces observed in the pure alcohols. The forces also increase with the content of methanol in the mixture, mirroring the increase in hydrogen bonding with methanol concentration, as seen in Figure 9. While the MD simulations show that the alcohols are less densely packed than water at the interface, so that the forces required to disrupt the hydrogen bond network are smaller, there nonetheless appears to be a strong correlation between the adhesive forces observed and the degree of hydrogen bonding taking place at the interface. This correlation is present regardless of the handedness of the enantiomer coating the tip.

4. Conclusions

In chromatography the choice of solvent is critical for achieving a desired separation. A typical separation employs a binary or ternary solvent. The objective of the present article is to examine in detail the characteristics of a binary solvent near a complex chiral interface. Specifically, we have described the solvation of the PEPU chiral stationary phase using a combination of experimental and theoretical methods. The PEPU molecule, like many others commonly used to build stationary phases for chiral chromatography, contains an aromatic ring and hydrogen bond sites. The PEPU interface is primarily hydrophobic, with phenyl rings at the surface. However, when cavities are included in the model surface, water or alcohols will descend into the cavity and hydrogen bond with the urea segments.[11]

In this article, MD simulations are used to explore the distribution and orientation of water and alcohol molecules at the interface and to quantify the degree of hydrogen bonding. Experimental (chemical force spectrometric) measurements were used to explore the adhesive interactions between two PEPU surfaces as a function of solvent composition. The MD simulations showed that, for methanol/water, 1-propanol/water, or 2-propanol/water mixtures, all the alcohols formed domains at the interface with the hydrophobic portions of the molecule tending to orient toward the surface. This effect disrupts the water hydrogen bonding networks at the interface and leads to the exclusion of water from the surface region relative to the bulk.

We show that the most important component in the interaction between the PEPU-modified tip and PEPU-modified substrate is the breaking of hydrogen bonds near the surface. Force spectrometric measurements of the adhesive interaction between two PEPU surfaces show that for 1- or 2-propanol, the adhesive interaction is rapidly suppressed with increasing alcohol concentration. This effect is less marked for methanol/water mixtures, consistent with the MD simulations that showed water less strongly excluded from the surface region in this system, as well as increased hydrogen-bonding interactions between water and methanol as compared with 1- and 2-propanol. Measurements in which the solvent consisted of methanol/1-propanol mixtures showed only a modest increase in adhesive force with increasing methanol concentration.

A complete description of the mechanism of selectivity for chiral interfaces must include a detailed representation of the surface and of the solvent at the interface. Together, force measurements and simulations are capable of providing the detailed level of description necessary to fully understand these complex interfaces. Examination of other chiral stationary phases is currently under way.

Acknowledgment. The financial support of the Natural Sciences and Engineering Research Council of Canada is gratefully acknowledged.

Supporting Information Available: Table showing details of the PEPU simulations. This material is available free of charge via the Internet at http://pubs.acs.org.

References and Notes

(1) Price, W. S.; Ide, H.; Arata, Y. *J. Phys. Chem. A* **2003**, *107*, 4784.
(2) D'Angelo, M.; Onori, G.; Santucci, A. *J. Chem. Phys.* **1994**, *100*, 3107.
(3) Koga, Y.; Nishikawa, K.; Westh, P. *J. Phys. Chem. A* **2004**, *108*, 3873.
(4) Dixit, S.; Soper, A. K.; Finney, J. L.; Crain, J. *Europhys. Lett.* **2002**, *59*, 377.
(5) Jorgensen, W. L. *J. Phys. Chem.* **1986**, *90*, 1276.
(6) Jorgensen, W. L. *J. Am. Chem. Soc.* **1980**, *102*, 543.
(7) Noskov, S. I.; Lamoureux, G.; Roux, B. *J. Phys. Chem. B* **2005**, *109*, 6705.
(8) Dixit, S.; Poon, W. C. K.; Finney, J. L.; Soper, A. K. *Nature* **2002**, *416*, 829.
(9) Fidler, J.; Rodger, P. M. *J. Phys. Chem.* **1999**, *103*, 7695.
(10) Laaksonen, A.; Kusalik, P. G.; Svishchev, I. M. *J. Phys. Chem. A* **1997**, *101*, 5910.
(11) Nita, S.; Cann, N. M.; Horton, J. H. *J. Phys. Chem. B* **2004**, *108*, 3512.
(12) Wainer, I. W. *Trends Anal. Chem.* **1987**, *6*, 135.
(13) Capka, M.; Bartlova, M.; Krause, H. W.; Schmidt, U.; Fischer, C.; Oehme, G. *Am. Biotechnol. Lab.* **1995**, *13*, 13.
(14) Dyas, A. M.; Robinson, M. L.; Fell, A. F. *Chromatographia* **1990**, *30*, 73.
(15) Lipkowitz, K. B. *J. Chromat. A* **2001**, *906*, 417.
(16) Lipkowitz, K. B. J. *Chromat. A* **1995**, *694*, 15.
(17) Lipkowitz, K. B. *J. Chromat. A* **1994**, *666*, 493.
(18) Booth T. D.; Azzaoui K.; Wainer I. W. *Anal. Chem.* **1997**, *69*, 3879.
(19) Wolf R. M.; Francotte E.; Lohmann D. *J. Chem. Soc., Perkin Trans.* **1988**, *2*, 893.
(20) Wallwork, M. L.; Smith, D. A.; Zhang, J.; Kirkham, J.; Robinson, C. *Langmuir* **2001**, *17*, 1126.
(21) Skulason, H.; Frisbie, C. D. *J. Am. Chem. Soc.* **2002**, *124*, 15125.
(22) *CRC Handbook of Chemistry and Physics*, 85th ed.; Lide, D. R., Ed.; CRC Press: Boca Raton, FL 2005.
(23) Sader, J. E. *Rev. Sci. Instrum.* **1995**, *66*, 4583.
(24) Sader, J. E. *J. Appl. Phys.* **1998**, *84*, 64.
(25) Sader, J. E.; Chon, J. W. M.; Mulvaney, P. *Rev. Sci. Instrum.* **1999**, *70*, 3967.
(26) Green, C. P.; Lioe, H.; Cleveland, J. P.; Proksch, R.; Mulvaney, P.; Sader, J. E. *Rev. Sci. Instrum.* **2004**, *75*, 1988.
(27) Frisch M. J.; Trucks, G. W.; Schlegel, H. B.; Scuseria, G. E.; Robb, M. A.; Cheeseman, J. A.; Zakrzewski, V. G.; Montgomery, J. A., Jr.; Stratmann, R. E.; Burant, J. C.; Dapprich, S.; Millam, J. M.; Daniels, A. D.; Kudin, K. N.; Strain, M. C.; Farkas, O.; Tomasi, J.; Barone, V.; Cossi, M.; Cammi, R.; Mennucci, B.; Pomelli, C.; Adamo, C.; Clifford, S.; Ochterski, J.; Petersson, G. A.; Ayala, P. Y.; Cui, Q.; Morokuma, K.; Malick, D. K.; Rabuck, A. D.; Raghavachari, K.; Foresman, J. B.; Cioslowski, J.;

Ortiz, J. V.; Baboul, A. G.; Stefanov, B. B.; Liu, G.; Liashenko, A.; Piskorz, P.; Komaromi, I.; Gomperts, R.; Martin, R. L.; Fox, D. J.; Keith, T.; Al-Laham, M. A.; Peng, C. Y.; Nanayakkara, A.; Challacombe, M.; Gill, P. M. W.; Johnson, B.; Chen, W.; Wong, M. W.; Andres, J. L.; Gonzalez, C.; Head-Gordon, M.; Replogle, E. S.; Pople, J. A. *Gaussian 98*, revision A.9; Gaussian, Inc., Pittsburgh, PA, 1998.

(28) Levitt, M.; Hirshberg, M.; Sharon, R.; Laidig, K. E.; Daggett, V. *J. Phys. Chem. B* **1997**, *101*, 5051.

(29) Armen, R. S.; Daggett, V. *Biochemistry* **2005**, *44*, 16098.

(30) Esposito, L.; Daggett, V. *Biochemistry* **2005**, *44*, 3358.

(31) Dougan, L.; Hargreaves, R.; Bates, S. P.; Finney, J. L.; Reat, V.; Soper, A. K.; Crain, C. *J. Chem. Phys.* **2005**, *122*, 174514.

(32) Dougan, L.; Hargreaves, R.; Bates, S. P.; Hargreaves, R.; Fox, J. P.; Crain, J.; Finney, J. L.; Reat, V.; Soper, A. K. *J. Chem. Phys.* **2004**, *121*, 6456.

(33) Allison, S. K.; Fox, J. P.; Hargreaves, R.; Bates, S. P. *Phys. Rev. B* **2005**, *71*, 024201.

(34) Ju, S. P.; Chang, J. G.; Lin, J. S.; Lin, Y. S. *J. Chem. Phys.* **2005**, *122*, 154707.

(35) Ju, S. P. *J. Chem Phys.* **2005**, *122*, 094718.

(36) Wu, Y.; Tepper, H. L.; Voth, G. A. *J. Chem. Phys.* **2006**, *124*, 024503.

(37) Beck, D. A. C.; Armen, R. S.; Daggett, V. *Biochemistry* **2005**, *44*, 609.

(38) Chen, B.; Potoff, J. J.; Siepmann, J. I. *J. Phys. Chem. B* **2001**, *105*, 3093.

(39) Wick, C. D.; Siepmann, J. I.; Schure, M. R. *Anal. Chem.* **2004**, *76*, 2886.

(40) Chen, B.; Siepmann, J. I.; Klein, M. L. *J. Am. Chem. Soc.* **2003**, *125*, 3113.

(41) Shelley, J. C.; Patey, G. N. *Mol. Phys.* **1996**, *88*, 385.

(42) Ewald, P. P. *Ann. Phys.* **1921**, *64*, 253.

(43) Wasburn, E. W.; Ed. *International Critical Tables of Numerical Data, Physics, Chemistry and Technology*; Knovel, NY, 2003.

(44) Hoover, W. G. *Phys. Rev. A* **1985**, *31*, 1695.

(45) Martyna, G. J.; Klein, M. L.; Tuckerman, M. *J. Chem. Phys.* **1992**, *97*, 2635.

(46) Cressman E.; Das B.; Dunford J.; Ghenea R.; Huh Y.; Nita S.; Paci I.; Wang. S.; Zhao C.; Cann, N. M. unpublished.

(47) De Loof, H.; Nilsson, L.; Rigler, R. *J. Am. Chem. Soc.* **1992**, *114*, 4028.

(48) Luzar, A.; Chandler, D. *Phys Rev. Lett.* **1996**, *76*, 928.